

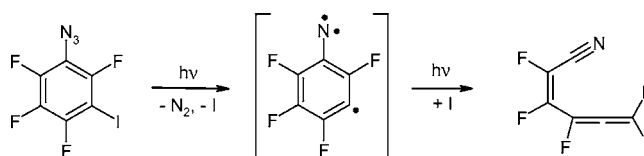
Dehydrophenylnitrenes: Matrix Isolation and Photochemical Rearrangements

Wolfram Sander,* Michael Winkler, Bayram Cakir, Dirk Grote, and Holger F. Bettinger

Lehrstuhl für Organische Chemie II, Ruhr-Universität Bochum, Universitätsstrasse 150,
44780 Bochum, Germany

wolfram.sander@rub.de

Received August 4, 2006



The photochemistry of 3-iodo-2,4,5,6-tetrafluorophenyl azide **8** and 3,5-diiodo-2,4,6-trifluorophenyl azide **9** was studied by IR and EPR spectroscopy in cryogenic argon and neon matrices. Both compounds form the corresponding nitrenes as primary photoproducts in photostationary equilibria with their azirine and ketenimine isomers. In contrast to fluorinated phenylnitrenes, ring-opened products are obtained upon short-wavelength irradiation of the iodine-containing systems, indicative of C–I bond cleavage in the nitrenes or didehydroazepines under these conditions. Neither 3-dehydrophenylnitrene **6** nor 3,5-didehydrophenylnitrene **7** could be detected directly. The structures of the acyclic photoproducts were identified by extensive comparison with DFT calculated spectra. Mechanistic aspects of the rearrangements leading to the observed products and the electronic properties of the title intermediates are discussed on the basis of DFT as well as high-level ab initio calculations. The computations indicate strong through-bond coupling of the exocyclic orbital in the *meta* position with the singly occupied in-plane nitrene orbital in the monoradical nitrenes. In contrast to the *ortho* or *para* isomers, this interaction results in low-spin ground states for *meta* nitrene radicals and a weakening of the C1–C2 bond causing the kinetic instability of these species even under low-temperature conditions. 3,5-Didehydrophenylnitrenes, on the other hand, in which a strong C3–C5 interaction reduces coupling of the radical sites with the nitrene unit, might be accessible synthetic targets if the intermediate formation of labile monoradicals could be circumvented.

Introduction

High-spin organic molecules are for both the experimentalist and theoretician challenging species with potential applications for the development of new magnetic materials. An important and successful approach for achieving high-spin states is via π -coupling in non-Kekulé molecules.¹ In particular *m*-phenylene units have proved to be reliable linkers for generating high-spin states of polyradicals,² -carbenes,^{3–5} and -nitrenes.^{6,7} In contrast, *para* or *ortho* coupling of π -radicals, carbenes, or

nitrenes results in low-spin, quinoid arrangements. Lahti et al. described the formation of the quartet ground state molecules **1** and **2** via coupling of a phenylnitrene unit with a stable π -radical attached to the *para* position of the phenyl ring.^{8,9} The three unpaired electrons of these spin systems consist of one σ -electron localized at the nitrene center, one delocalized nitrene π -electron, and one delocalized radical π -electron ($\sigma\pi\pi$ triradical). Spin fragment analysis reveals the non-disjoint nature of these spin systems and consequently the high spin (quartet)

(1) Berson, J. A. In *Reactive Intermediate Chemistry*; Moss, R. A., Platz, M. S., Jones, M., Jr., Eds.; Wiley: New York, 2004.

(2) Lahti, P. M.; Liao, Y.; Julier, M.; Palacio, F. *Synth. Met.* **2001**, *122* (3), 485.

(3) Sato, K.; Shiomi, D.; Takui, T.; Hattori, M.; Hirai, K.; Tomioka, H. *Mol. Cryst. Liq. Cryst. Sci. Technol., Sect. A* **2002**, *376*, 549.

(4) Teki, Y.; Itoh, K. *Magn. Prop. Org. Mater.* **1999**, 237.

(5) Itoh, K. In *NATO ASI Ser., Ser. E* **1991**, *198*, 67.

(6) Chapyshev, S. V.; Walton, R.; Sanborn, J. A.; Lahti, P. M. *J. Am. Chem. Soc.* **2000**, *122*, 1580.

(7) Sato, T.; Narazaki, A.; Kawaguchi, Y.; Niino, H.; Bucher, G.; Grote, D.; Wolff, J. J.; Wenk, H. H.; Sander, W. *J. Am. Chem. Soc.* **2004**, *126*, 7846.

(8) Lahti, P. M.; Esat, B.; Liao, Y.; Serwinski, P.; Lan, J.; Walton, R. *Polyhedron* **2001**, *20*, 1647.

(9) Serwinski, P. R.; Esat, B.; Lahti, P. M.; Liao, Y.; Walton, R.; Lan, J. *J. Org. Chem.* **2004**, *69*, 5247.

CHART 1

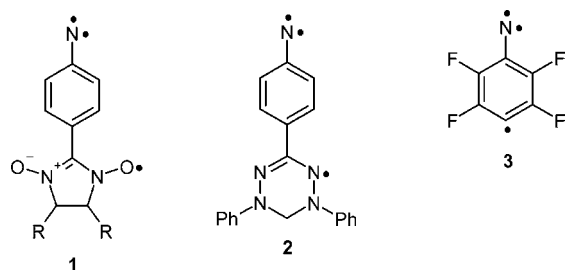
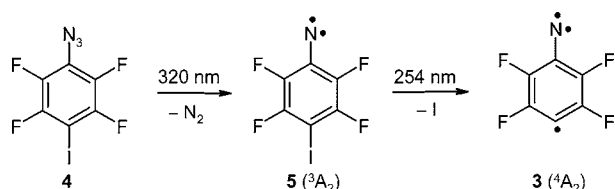


CHART 2



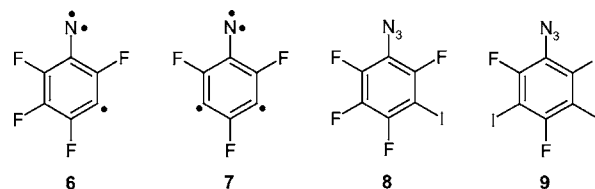
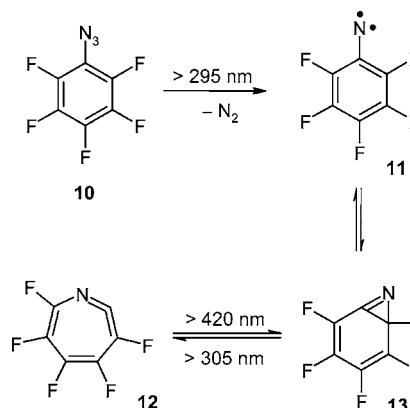
ground states that have been observed via EPR spectroscopy.⁹ Recently, we described a novel high-spin molecule **3** with a quartet ground state formed by *para* coupling of a phenylnitrene unit and a phenyl radical center.¹⁰ In this system, one π -electron is coupled to two σ -electrons located formally at the nitrogen atom and the *p*-phenyl carbon atom, respectively ($\sigma\pi\sigma$ tri-radical).

4-Iodo-2,3,5,6-tetrafluorophenyl azide **4** was used as photochemical precursor of **3**. Azides are versatile nitrene precursors, and aryl iodides with a rather labile C–I bond can be used to generate phenyl radicals. A major problem of aryl iodides as precursors of radicals in matrices is the rapid thermal recombination of the photochemically generated phenyl radicals and the iodine atoms residing in the same matrix cages. This in-cage recombination is suppressed if the radical pairs are separated by inert gas atoms in the rigid matrix. The yield of matrix-isolated radicals depends on the constitution of the radical precursor, on the matrix material, and on the matrix temperature. Fluorine substitution at the phenyl rings has been shown to increase the yield of radicals after irradiation in matrices.¹¹

As expected, 320 nm photolysis of **4**, matrix isolated in argon at 3 K, produced triplet ground state nitrene **5** as the primary photoproduct.¹⁰ Subsequent 254 nm photolysis resulted in the formation of 2,3,5,6-tetrafluorophenyl nitrene-4-yl **3** with a quartet ground state.^{10,12} The nitrene radical was identified by comparison of the matrix IR spectrum with spectra calculated for the lowest lying doublet and quartet states, where the latter gives a better agreement with the experimental data than the doublet spectrum.¹⁰ The assignment of a quartet ground state to phenylnitrene radical **3** was later confirmed by EPR measurements.¹³ The nitrene radical **3** represents the first example of a novel coupling between a σ -radical and a nitrene unit resulting in a high-spin state.¹²

According to our calculations, a *meta* coupling between the phenyl radical and the nitrogen atom should lead to a low-spin doublet configuration of the resulting phenylnitrene radical.¹² It is thus tempting to investigate the corresponding 2,4,5,6-tetrafluorophenyl nitrene-3-yl **6**. Another interesting system is

CHART 3

SCHEME 1. Photochemistry of Pentafluorophenyl Azide **10**, Matrix Isolated in Argon at 10 K

the 2,4,6-trifluorophenyl nitrene-3,5-diyl **7** with the two radical and the nitrene centers in the *meta* position, which combines a phenylnitrene with a *m*-benzylidene unit. Here we describe the photochemistry of the phenyl azides **8** and **9** as potential precursors of the phenylnitrene radicals **6** and **7**, respectively, under the conditions of matrix isolation.

Results and Discussion

Photochemistry of Pentafluorophenyl Azide 10. Phenylnitrenes are photolabile and on UV irradiation rearrange to azirines which on subsequent irradiation produce cyclic ketenimines (didehydroazepines).¹⁴ These rearrangements are reversible, and thus under the conditions of matrix isolation photostationary equilibria between these three reactive intermediates are observed. Pentafluorophenyl nitrene **11** was first matrix isolated and spectroscopically characterized by Dunkin et al. describing it as “an aryl nitrene that does not undergo ring expansion”.^{14c} Later, we found azirine **13** as a reversibly formed photoproduct of nitrene **11**.¹⁵ Again, ring expansion of nitrene **11** was not observed. Only recently, Bally et al.¹⁶ reported for the related 2,6-difluorophenyl nitrene that the missing didehydroazepine is indeed formed if monochromatic UV light is used in the irradiation of 2,6-difluorophenyl nitrene. Since fluorinated didehydroazepines, such as **12**, are labile toward visible light irradiation ($\lambda > 420$ nm) they are not observed if broadband UV–vis irradiation is used to irradiate the nitrene. The relative yields of the three reactive intermediates **11**–**13** strongly depend on the irradiation conditions. However, even prolonged short-

(14) (a) Dunkin, I. R.; Thomson, P. C. *J. Chem. Soc., Chem. Commun.* **1982**, 1192. (b) Hayes, J. C.; Sheridan, R. S. *J. Am. Chem. Soc.* **1990**, *112*, 5879. (c) Borden, W. T.; Gritsan, N. P.; Hadad, C. M.; Karney, W. L.; Kennitz, C. R.; Platz, M. S. *Acc. Chem. Res.* **2000**, *33*, 765. (d) Platz, M. S. In *Reactive Intermediate Chemistry*; Moss, R. A., Platz, M. S., Jones, M., Jr., Eds.; Wiley: New York, 2004.

(15) Morawietz, J.; Sander, W. *J. Org. Chem.* **1996**, *61*, 4351.

(16) Carra, C.; Nussbaum, R.; Bally, T. *Chem. Phys. Chem.* **2006**, *7*, 1268.

(10) Wenk, H. H.; Sander, W. *Angew. Chem., Int. Ed.* **2002**, *41*, 2742.

(11) (a) Wenk, H. H.; Sander, W. *Eur. J. Org. Chem.* **1999**, *57*. (b) Wenk, H. H.; Sander, W. *Chem. Eur. J.* **2001**, *7*, 1837.

(12) Bettinger, H. F.; Sander, W. *J. Am. Chem. Soc.* **2003**, *125*, 9726.

(13) Grote, D.; Wenk, H. H.; Sander, W. Unpublished results.

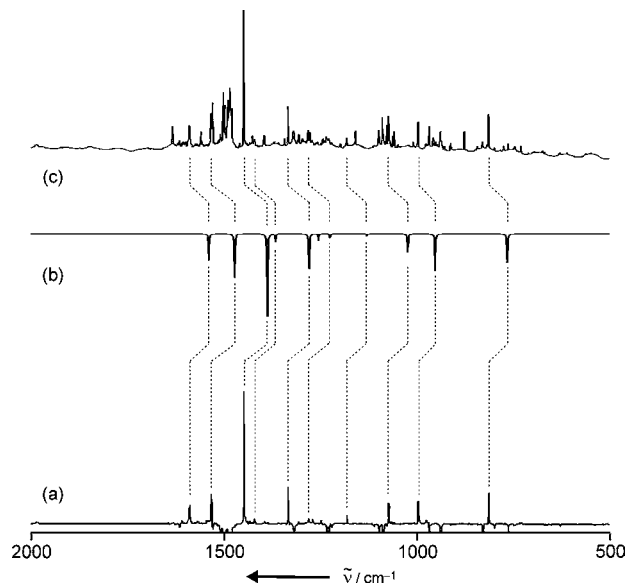


FIGURE 1. Photochemistry of 3-iodo-2,4,5,6-tetrafluorophenyl azide **8**, matrix-isolated in neon at 3 K. (a) Difference IR spectrum of a matrix obtained after short-time photolysis of **8** at $\lambda = 305\text{--}320$ nm. (b) Calculated IR spectrum of triplet nitrene **14**. (c) IR spectrum of the same matrix as in part a after prolonged irradiation. A complex mixture of **8**, **14**, and **15** is obtained. Note that no **16** is formed under these conditions.

wavelength UV irradiation (248 nm Excimer Laser) does not lead to ring-opened acetylenic compounds.¹⁷ This is in contrast to the chemistry of the phenylnitrenes containing one or two iodine atoms described in the next section.

Photochemistry of 3-Iodo-2,4,5,6-tetrafluorophenyl Azide

8. UV photolysis of azide **8**, matrix isolated in argon at 10 K, with $\lambda = 305\text{--}320$ (high-pressure mercury arc lamp and cutoff filters) or 308 nm (XeCl Excimer laser) produced 2,4,5,6-tetrafluoro-3-iodophenylnitrene **14** with an EPR spectrum characteristic of triplet nitrenes. By simulation of the EPR spectra the zero field splitting parameters (ZFS) $D/h\nu$ and $E/h\nu$ were determined to be 1.033 and 0.039 cm^{-1} , respectively.

Using matrix IR spectroscopy to analyze the photolysis of **8** reveals a more complex reaction pattern. The experiments were performed both in argon at 10 K and in neon at 3 K with the latter showing a higher resolution of the IR spectra. Since otherwise the results from both matrices are identical, only the spectra in solid neon are discussed here. UV photolysis ($\lambda = 305\text{--}320$ nm) of **8** produced nitrene **14** with the most intense vibration at 1446 cm^{-1} . The measured IR spectrum of **14** agrees nicely with calculations at the BLYP/6-311G(d,p) level of theory (Figure 1, Table 1).

Prolonged irradiation at $\lambda > 305$ nm leads to the formation of several additional products that are identified as the dehydroazepines **15a** and **15b** and the azirines **16a** and **16b** (Scheme 2) by comparison with DFT calculated spectra (Table 1). Nitrene **14**, dehydroazepines **15**, and azirines **16** are formed in photo-stationary equilibria and the relative yields of these compounds strongly depend on the irradiation conditions. Similar to the pentafluoro derivative (vide supra), irradiation at $\lambda > 420$ nm

increases the concentration of azirines **16** at the expense of ketenimines **15** (Figure 2). To this point the photochemistry of **14** is in accordance with the photochemical isomerization of pentafluorophenylnitrene **11**.

Short-wavelength UV irradiation (248 nm KrF Excimer Laser or 254 nm low-pressure mercury arc lamp) results in the formation of two new products (Figure 3). The first product exhibits a weak absorption at 2286 cm^{-1} , which is characteristic of alkynes or nitriles. A medium intensity absorption at 1982 cm^{-1} is found in the region typical of allenes. The second product, formed upon prolonged irradiation, exhibits a very strong absorption at 2352 cm^{-1} . A comparison with calculated IR spectra of a large number of $\text{C}_6\text{F}_4\text{N}$ and $\text{C}_6\text{F}_4\text{NI}$ isomers allows us to tentatively assign the two compounds to allene **19** and its acetylene isomer **20** (Table 2). Calculated IR spectra of various other potential side products are given in the Supporting Information section for comparison. The nitrile absorption in **20** is predicted to be of very low intensity around 2250 cm^{-1} and is thus not observed experimentally. Obviously, short-wavelength irradiation results in the rupture of either the six- or seven-membered ring and formation of acyclic products. From the experimental data it is not possible to decide whether the ring opening involves **6** or **17**, or whether both pathways contribute to formation of acyclic products. Since the electronic properties of the fluorine and iodine substituents are roughly comparable, however, the different behavior of **11** and **14** upon short-wavelength UV irradiation suggests that cleavage of the C–I bond takes place at the stage of either **14** or **15**, and that recombination with iodine occurs after ring opening (Scheme 2).

To gain additional insight into the formation of acyclic photoproducts a number of isomers and reaction paths of nitrene radical **6** were calculated (Scheme 3). Although the vibrational spectra of these compounds are usually nicely reproduced at the DFT level, the doublet–quartet splittings and reaction barriers should be taken with some caution (vide infra). According to these calculations, **6** has a doublet ground state with a $^4\text{A}''$ state lying 10 kcal mol^{-1} above. This is in qualitative agreement with our previous calculations on the parent system.¹² The calculated barriers for rearrangement to azirines **21a** and **21b** are significantly higher, and the latter are less stable than expected by comparison with fluorinated phenylnitrenes that have been the subject of high-level experimental and computational studies.¹⁴ In further contrast to the latter, **21a** and **21b** occupy very shallow minima on the $\text{C}_6\text{F}_4\text{N}$ potential energy surface that disappear as stationary points when zero point vibrational energy (ZPVE) corrections are taken into account. The ketenimines **17a** and **17b** are more stable than **6** by 11 and 9 kcal mol^{-1} , respectively. As discussed in detail for the parent 3-dehydrophenylnitrene previously,¹² the C1–C2 bond of **6** is weakened by through-bond interaction¹⁸ of the exocyclic σ orbital in the *meta* position with the singly occupied in-plane orbital at nitrogen. Accordingly, rupture of this bond requires only a small barrier of 6 kcal mol^{-1} leading to the delocalized π -radical **18** that is 18 kcal mol^{-1} more stable than **6**. Alternatively, **17b** can undergo a ring-opening reaction to the same intermediate with a barrier of 10 kcal mol^{-1} . Whether this reaction is a real photochemical process, taking place on

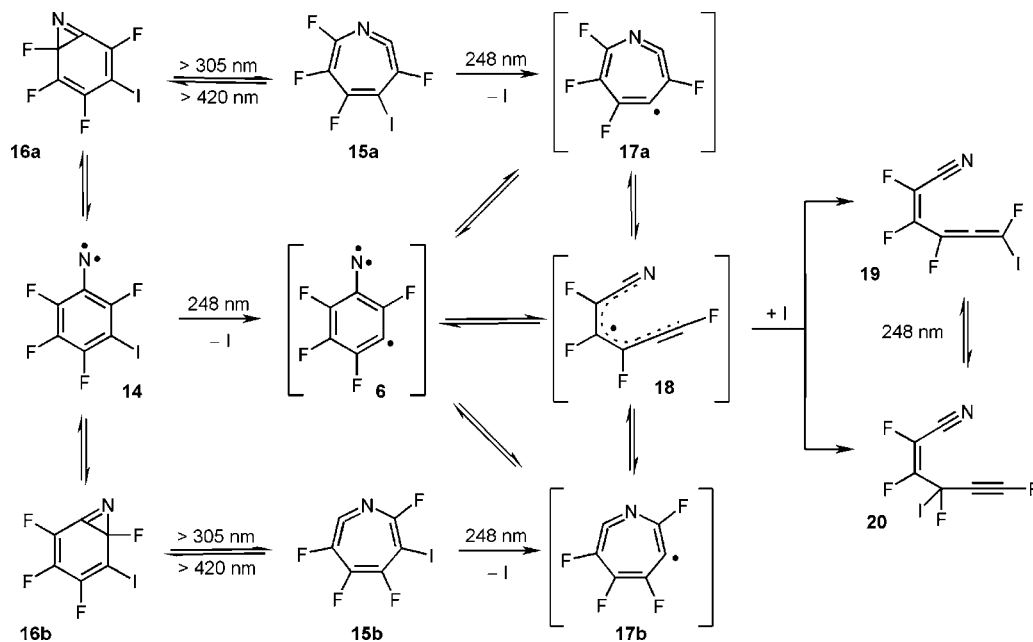
(17) In contrast to **11**, ring-opening reactions of annellated phenylnitrenes have been observed previously: (a) Maltsev, A.; Bally, T.; Tsao, M. L.; Platz, M. S.; Kuhn, A.; Vosswinkel, M.; Wentrup, C. *J. Am. Chem. Soc.* **2004**, *126*, 237. (b) Kvaskoff, D.; Bednarek, P.; George, L.; Waich, K.; Wentrup, C. *J. Org. Chem.* **2006**, *71*, 4049.

(18) For example: (a) Hoffmann, R.; Imamura, A.; Hehre, W. J. *J. Am. Chem. Soc.* **1968**, *90*, 1499. (b) Hoffmann, R. *Acc. Chem. Res.* **1971**, *4*, 1. (c) Gleiter, R. *Angew. Chem., Int. Ed.* **1974**, *13*, 696. (d) Paddon-Row, M. N. *Acc. Chem. Res.* **1982**, *15*, 245. (e) Jordan, K. *Theor. Chem. Acc.* **2000**, *103*, 286.

TABLE 1. IR Spectroscopic Data of 14, 15a, 15b, 16a, and 16b^c

14				15a				15b				16a				16b			
$\tilde{\nu}_{\text{exp}}^a$	$I_{\text{exp}}^{a,b}$	$\tilde{\nu}_{\text{calc}}^c$	I_{calc}^c	$\tilde{\nu}_{\text{exp}}^a$	$I_{\text{exp}}^{a,b}$	$\tilde{\nu}_{\text{calc}}^c$	I_{calc}^c	$\tilde{\nu}_{\text{exp}}^a$	$I_{\text{exp}}^{a,b}$	$\tilde{\nu}_{\text{calc}}^c$	I_{calc}^c	$\tilde{\nu}_{\text{exp}}^a$	$I_{\text{exp}}^{a,b}$	$\tilde{\nu}_{\text{calc}}^c$	I_{calc}^c	$\tilde{\nu}_{\text{exp}}^a$	$I_{\text{exp}}^{a,b}$	$\tilde{\nu}_{\text{calc}}^c$	I_{calc}^c
$\tilde{\nu}_{\text{exp}}$						406	1			447	5			402	3			414	3
		420	0			463	1			481	0			424	2			455	5
		481	7			529	8			525	11			518	6			539	13
		550	0			562	4			559	10			566	7			569	2
		573	3			597	3			576	1			599	9			581	3
		604	0			629	2			635	4			627	1			623	4
		634	0	672	50	648	69			650	5			662	0			664	1
		705	2	693	5	668	12	697	5	677	25	792	20	749	40	<i>d</i>	<i>d</i>	739	52
812	50	767	86	781	20	736	120	817	50	775	127	843	40	798	83	832	5	779	44
994	50	953	107	926	60	889	124	966	10	935	43	935	20	883	36	973	20	909	69
1071	40	1024	54	1046	60	1003	73	1007	80	960	210	1005	60	953	140	1019 ^d	<i>d</i>	971	99
1179	10	1130	10	1181	20	1126	42	1140	10	1076	17	1147 ^d	<i>d</i>	1084	107	1147 ^d	<i>d</i>	1089	126
1279 ^d	<i>d</i>	1227	14	<i>d</i>	<i>d</i>	1224	26	1255	<i>d</i>	1209	99	1210 ^d	<i>d</i>	1130	46	1210 ^d	<i>d</i>	1130	35
<i>d</i>	<i>d</i>	1257	20	1304	100	1246	406	1282	<i>d</i>	1227	108	1287 ^d	<i>d</i>	1223	101	1278	<i>d</i>	1206	32
1332	50	1280	104	<i>d</i>	<i>d</i>	1259	70	1324	<i>d</i>	1269	124	1320 ^d	<i>d</i>	1258	46	1313	<i>d</i>	1246	247
1419	10	1367	24	1357	40	1312	241	1393	100	1324	388	1375	<i>d</i>	1314	261	1386	100	1316	210
1446	100	1388	237	1531	<i>d</i>	1453	203	1524	<i>d</i>	1445	93	<i>d</i>	<i>d</i>	1454	4	1547	20	1470	91
1531	50	1473	127	1586	<i>d</i>	1510	76	1586	<i>d</i>	1512	135	1615	100	1545	183	1642	40	1559	88
1587	40	1540	78	1845	<i>d</i>	1801	207	1872	20	1830	98	1696	<i>d</i>	1663	52	1696	<i>d</i>	1669	87

^a Ne, 3 K. ^b Relative intensity based on the strongest absorption. Due to the complexity of the spectra, all experimental intensities are rough estimates. ^c BLYP/6-311G(d,p). ^d Not assigned or tentative assignment because of overlap with other nearby bands. ^e Frequencies are given in cm⁻¹, calculated Intensities in km mol⁻¹.

SCHEME 2. Photochemistry of Nitrene 14, Matrix Isolated in Neon at 3 K^a

^a Since **11** is completely stable toward ring-opening upon short-wavelength irradiation, cleavage of the C–I bond in **14** or **15** prior to ring rupture is likely.

an excited-state potential energy surface, or a hot ground state reaction cannot be decided conclusively from our experiments. Anyway, the excess energy available from the photolytic generation of **6** or **17** cannot be dissipated easily in noble-gas matrices, and is more than sufficient to trigger the **6** → **18** rearrangement even in the ground state. Subsequent recombination of **18** with a nearby iodine atom accounts for the formation of ring-opened compounds **19** and **20** as shown in Scheme 2. Overall, the DFT calculations support the mechanistic interpretation of the experimental findings and indicate that **6** is kinetically labile toward ring-opening. In contrast to the *ortho*

and *para* isomers, these systems do not qualify as synthetic targets, even under low-temperature conditions.

Photochemistry of 3,5-Diiodo-2,4,6-trifluorophenyl Azide 9. Matrix-isolated azide **9** was irradiated under conditions analogous to those of the photolysis of **8** described above. The photochemistry of **9** proved to be much cleaner than that of **8**. As with the other phenyl azides the primary photoproduct is the corresponding nitrene **22**. The nitrene was characterized by its EPR and IR spectra. The EPR spectrum is characteristic for a triplet nitrene with the ZFS parameters $D/h\nu$ and $E/h\nu$ of 1.012 and 0.094 cm⁻¹, respectively. The IR spectrum of **22** shows

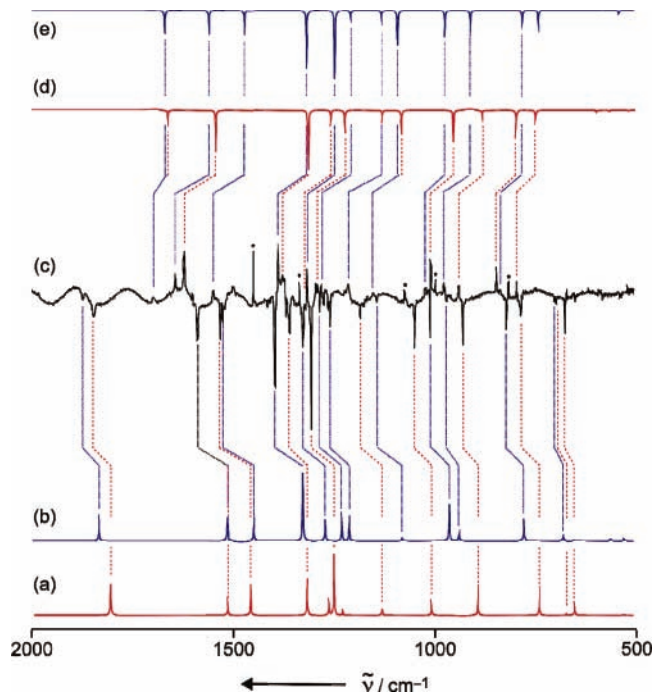


FIGURE 2. Interconversion of didehydroazepines **15** to azirines **16** upon irradiation with visible light. (a) Calculated IR spectrum of **15a**. (b) Calculated IR spectrum of **15b**. (c) Difference IR spectrum (neon, 3 K) of a matrix obtained after irradiation of **8** with $\lambda > 305$ nm followed by irradiation at $\lambda > 420$ nm. Bands pointing upwards increase in intensity upon long-wavelength irradiation. Absorptions of **14** are labeled by dots. (d) Calculated IR spectrum of **16a**. (e) Calculated IR spectrum of **16b**.

strong absorptions at 1536, 1416, and 1303 cm^{-1} and is nicely reproduced by DFT calculations (Table 3, Figure 4).

Further irradiation of **22** with 254 or 308 nm UV light resulted in the formation of only two major new products which were characterized by IR spectroscopy. One of the products exhibits a strong absorption at 1852 cm^{-1} characteristic of ketenimines and was identified as 1,2-didehydro-3,5,7-trifluoro-4,6-di-iodoazepine **23** (Table 3, Figure 4). Presumably azirine **24** is the precursor of **23**; however, it could not be directly observed in our experiments.

The second product is formed almost exclusively on prolonged irradiation and shows intense absorptions at 2333, 1995, 1174, 1081, and 854 cm^{-1} . The band at 1995 cm^{-1} of the second photoproduct is characteristic of an allene, and by comparison with the results from DFT calculations this compound was identified as 2,4,6-trifluorohexa-2,3-dien-5-yne nitrile **25** (Figure 5). Obviously, ring cleavage is a highly efficient process in this system as well (Scheme 4), and no evidence for the formation of **7** could be obtained by IR or EPR spectroscopy.

In analogy to the 3-iodo-tetrafluoro system, we also investigated the ring fragmentation of **7** at the DFT level. Since density functional theory erroneously predicts a singlet ground state for nitrene **7**, the DFT calculated energetics for the ring-opening process $7 \rightarrow 27$ should be considered as tentative only. According to these calculations, the rearrangement on the triplet potential energy surface requires an energy of 14.3 kcal mol^{-1} , and the reaction is less exothermic (-11.6 kcal mol^{-1}) than the $6 \rightarrow 18$ rearrangement. Thus, the kinetic stability of **7** is significantly higher than that of monoradical **6**.

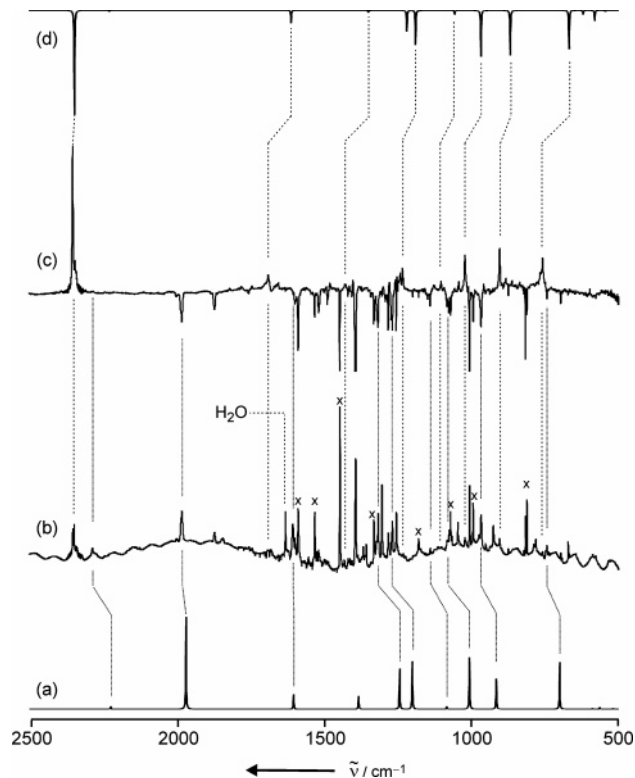


FIGURE 3. Formation of ring-opened compounds **19** and **20** upon irradiation at 248 nm. (a) Calculated IR spectrum of **19**. (b) IR spectrum of a matrix obtained after irradiation of **8** with 305–320 nm, followed by short-time irradiation at 248 nm. (c) Difference IR spectrum of the same matrix after continued irradiation at 248 nm. Bands pointing upwards increase in intensity upon prolonged irradiation. Absorptions of **14** are labeled by crosses for comparison. Most of the remaining bands belong to **15**. (d) Calculated IR spectrum of **20**.

TABLE 2. IR Spectroscopic Data of **19** and **20**^e

19				20			
$\tilde{\nu}_{\text{exp}}^a$	$I_{\text{exp}}^{a,b}$	$\tilde{\nu}_{\text{calc}}^c$	I_{calc}^c	$\tilde{\nu}_{\text{exp}}^a$	$I_{\text{exp}}^{a,b}$	$\tilde{\nu}_{\text{calc}}^c$	I_{calc}^c
		455	2				
		477	3				
		519	5			491	21
		565	10			537	1
		589	7			547	7
		603	2			583	46
		662	3			621	20
		702	229	759	60	669	160
		916	149	905	80	868	185
	<i>d</i>	1007	252	1022	70	969	189
		1084	15	1102	10	1057	19
		1201	232	1279	40	1189	142
	80	1245	196	<i>d</i>	<i>d</i>	1220	86
		1384	66	1401	10	1350	13
	70	1604	71	1689	30	1612	54
	100	1970	442			2229	8
	10	2225	15	2352	100	2346	423

^a Ne, 3 K. ^b Relative intensity based on the strongest absorption. Due to the complexity of the spectra, all experimental intensities are rough estimates. ^c BLYP/6-311G(d,p). ^d Not assigned or tentative assignment because of overlap with other nearby bands. ^e Frequencies are given in cm^{-1} , calculated intensities in km mol^{-1} .

To verify a triplet ground state of this system, and to rationalize the higher barrier for ring-opening, we investigated the electronic structure of **28** as a model for nitrene **7** in more detail. A closer examination of substituent effects in these and

SCHEME 3. Energetics of Different Rearrangements of Nitrene Radical 6 Calculated at the UBLYP/6-311G(d,p) Level of Theory

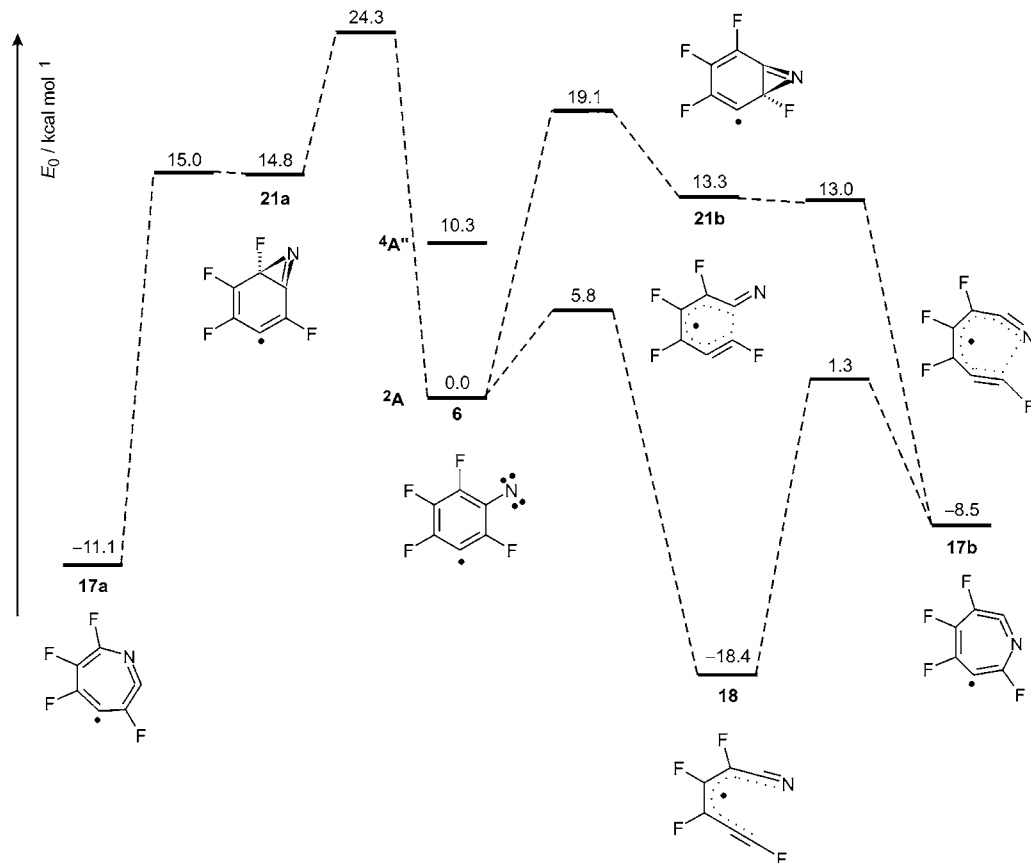


TABLE 3. IR Spectroscopic Data of 22, 23, and 25^d

22				23				25			
$\tilde{\nu}_{\text{exp}}^a$	$I_{\text{exp}}^{a,b}$	$\tilde{\nu}_{\text{calc}}^c$	I_{calc}^c	$\tilde{\nu}_{\text{exp}}^a$	$I_{\text{exp}}^{a,b}$	$\tilde{\nu}_{\text{calc}}^c$	I_{calc}^c	$\tilde{\nu}_{\text{exp}}^a$	$I_{\text{exp}}^{a,b}$	$\tilde{\nu}_{\text{calc}}^c$	I_{calc}^c
		447	2			422	4				
		549	1			501	18				
		578	0			547	23				
		607	4	562	10	565	6			430	3
658	60	621	70	603	54	603	54			464	1
		662	1	625	2	625	2			494	11
		678	6	651	59	651	59			568	1
700	5	678	6	677	21	677	21			604	8
901	40	862	45	915	60	865	152			623	4
1051	30	1009	37	929	20	929	20			639	2
		1017	19	1027	20	982	49	854	40	822	254
1268	10	1224	16	1241	40	1194	29	1081	50	1005	237
1277	40	1237	48	1260	100	1210	204	1174	50	1098	197
1302	70	1262	92	1320	60	1263	253	1316	20	1258	56
1390	5	1342	6	1332	70	1271	50	1436	5	1412	19
1414	80	1370	106	1507	60	1431	129	1995	90	1977	394
		1419	9	1539	50	1473	119			2233	5
1536	100	1500	138	1852	80	1805	217	2333	100	2339	465

^a Ne, 3 K. ^b Relative intensity based on the strongest absorption. Due to the complexity of the spectra, all experimental intensities are rough estimates. ^c BLYP/6-311G(d,p). ^d Frequencies are given in cm^{-1} , calculated intensities in km mol^{-1} .

related systems will be given elsewhere. Following our previous study on dehydrophenylnitrenes,¹² the ground and low-lying excited states of **28** were studied by second-order perturbation

theory (MR-MP2),¹⁹ employing a complete active space self-consistent-field reference wave function (CASSCF).

The ground state structures of **28–31** calculated at the CASSCF level are given in Figure 6. The distance of the radical centers in **28** is very similar to that of *m*-benzyne **31**,²⁰ and the length of the C–N bond is almost identical with that of phenyl

(19) (a) Hirao, K. *Chem. Phys. Lett.* **1992**, *190*, 374. (b) Hirao, K. *Chem. Phys. Lett.* **1992**, *196*, 397. (c) Hirao, K. *Int. J. Quantum Chem.* **1992**, *S26*, 517. (d) Hirao, K. *Chem. Phys. Lett.* **1993**, *201*, 59.

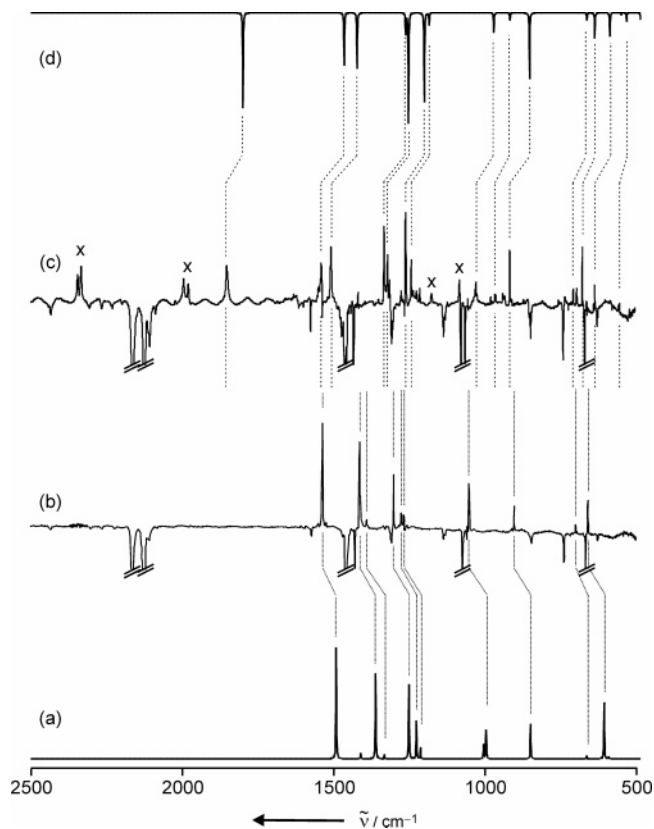


FIGURE 4. Photochemistry of azide **9** isolated in a neon matrix at 3 K. (a) Calculated IR spectrum of nitrene **22**. (b) Difference spectrum obtained after irradiation of the matrix at 305–320 nm. Bands pointing upwards increase in intensity after short-time irradiation. (c) Further photolysis leads to the formation of dihydroazepine **23**. Note that in this difference spectrum the concentration of **22** remains almost constant, i.e., the absorptions are very small, because it is formed and bleached at roughly the same rate until all **9** is consumed. Absorptions of allene **25** are labeled by crosses. (d) Calculated IR spectrum of dihydroazepine **23**.

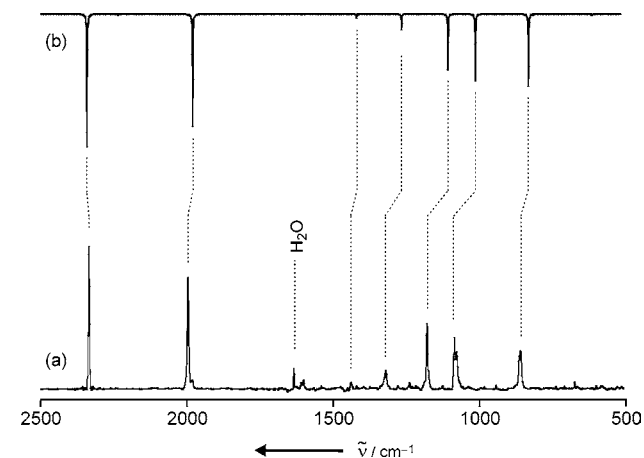


FIGURE 5. (a) IR spectrum of **25** generated by long-time irradiation (λ 305–320 nm) of **9**, matrix-isolated in neon at 3 K. (b) Calculated IR spectrum of allene **25**.

nitrene **30**. Most importantly, the C(N)–C(H) bonds in **28** are only modestly lengthened compared with **30**, indicating that through-bond interaction of the exocyclic orbitals at carbon with the nitrogen in-plane p orbital is much weaker than that in **29**.

This conclusion is further supported by the computed

SCHEME 4. Photochemistry of **9** Leading via Nitrene **22** Finally to Allene **25**

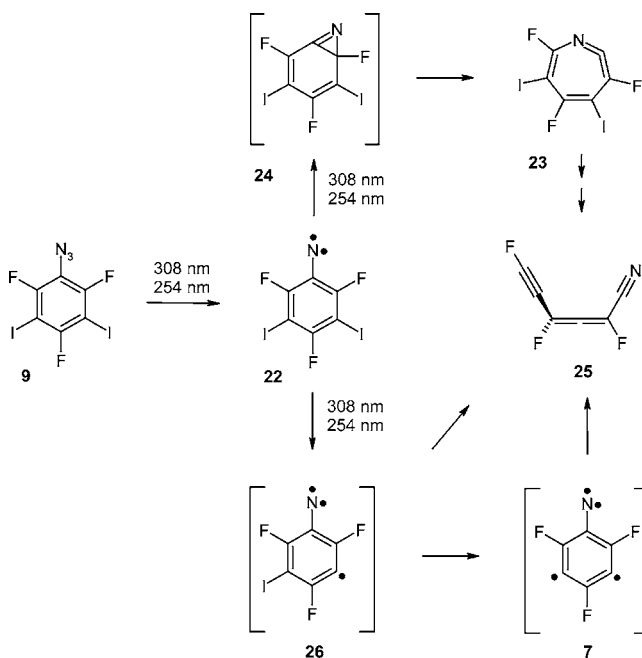


CHART 4

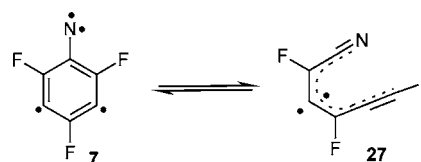
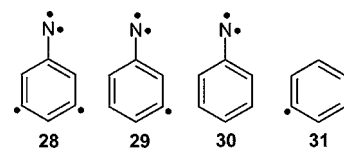


CHART 5



excitation energies of **28** given in Table 4. The first excited singlet state is of A_2 symmetry and 16.6 kcal mol⁻¹ above the 3A_2 ground state. It corresponds to the first excited singlet state of **30** for which a very similar singlet–triplet energy splitting (18.0 kcal mol⁻¹) is found at the same level of theory.¹² The next state of **28** is the 3B_1 triplet that is 17.5 kcal mol⁻¹ above the ground state, and which can be looked upon as the 3B_2 triplet state of *m*-benzynes **31** interacting with 3A_2 -**30**. For the former, a singlet–triplet gap of 21.3 kcal mol⁻¹ is found at the MR-MP2 level. Similar to the coupling in **29**, in 3B_1 -**28** there is strong interaction of the two, now uncoupled, electrons of the *m*-benzynes moiety with the in-plane nitrene p orbital, reducing the 3A_2 – 3B_1 gap of **28** as compared to the 1A_1 – 3B_2 splitting in **31**. Accordingly, the C(N)–C(H) bonds in 3B_1 -**28** are again considerably longer (143.8 pm), and the C–N bond is shorter (131.5 pm) than in the ground state. The lowest quintet state of

(20) (a) Sander, W. *Acc. Chem. Res.* **1999**, *32*, 669. (b) Winkler, M.; Sander, W. *J. Phys. Chem. A* **2001**, *105*, 10422. (c) Sander, W.; Exner, M.; Winkler, M.; Balster, A.; Hjerpe, A.; Kraka, E.; Cremer, D. *J. Am. Chem. Soc.* **2002**, *124*, 13072. (d) Wenk, H. H.; Winkler, M.; Sander, W. *Angew. Chem., Int. Ed.* **2003**, *42*, 502. (e) Winkler, M.; Cakir, B.; Sander, W. *J. Am. Chem. Soc.* **2004**, *126*, 6135.

(21) As with the iodotetrafluoro system, a pathway involving tri- or tetrahydroazepines cannot be excluded.

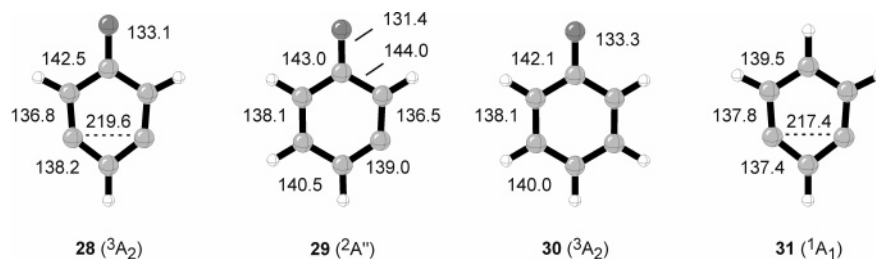


FIGURE 6. Structures of **28**–**31** calculated at the CASSCF/cc-pVTZ level of theory. Heavy-atom bond lengths are given in pm.

TABLE 4. Absolute (au), Relative (kcal mol⁻¹), Zero-Point Vibrational Energies (kcal mol⁻¹), and Number of Imaginary Vibrational Frequencies (Nimag) for Various Electronic States of 3,5-Didehydrophenylnitrene **28** as Computed at the CASSCF(10,10)/cc-pVTZ and MRMP2/cc-pVTZ//CASSCF(10,10)/cc-pVTZ Levels of Theory

state	CASSCF(10,10)	ZPVE (Nimag)	MR-MP2
³ A ₂	-283.40191	42.5 (0)	-284.38119
³ B ₁	12.4	na ^a	17.5
¹ A ₂	17.2	41.7 (0)	16.6
⁵ B ₁	18.1	42.8 (0)	24.8
¹ A ₁	38.6	na ^a	25.4

^a Not available.

28 is already 24.8 kcal mol⁻¹ above the ground state, and will not be discussed in detail here. Overall, ³A₂-**28** can be looked upon as a phenylnitrene, interacting only weakly with a separate *m*-benzyne moiety on the opposite side of the ring. The weakness of through-bond coupling compared to the strong C3–C5 interaction accounts for the higher kinetic stability of **28** found at the DFT level. On the basis of these arguments, and given the photolability of **6**, it is plausible to assume that the ring-opening observed experimentally occurs already at the stage of nitrene radical **26**.²⁰ In contrast to 3-dehydrophenylnitrenes, 3,5-didehydrophenylnitrenes might be accessible under low-temperature conditions, if precursors can be found that avoid the intermediate formation of the labile *m*-dehydrophenylnitrenes.

Conclusions

The photochemistry of 3-iodo-2,4,5,6-tetrafluorophenyl azide **8** and 3,5-diiodo-2,4,6-trifluorophenyl azide **9** was investigated in cryogenic argon and neon matrices, and compared to that of pentafluorophenyl azide **10**. All three compounds produce the corresponding nitrenes as primary photoproducts in photostationary equilibria with their azirine and didehydroazepine isomers. Only the iodine-containing systems undergo a ring-opening reaction upon prolonged irradiation with UV light, indicating that cleavage of the C–I bond occurs under these conditions. Neither 3-dehydrophenylnitrene **6** nor 3,5-didehydrophenylnitrene **7** could be detected by IR or EPR spectroscopy. According to DFT and ab initio computations, the 3-dehydrophenylnitrenes are labile systems that rapidly undergo a ring-opening reaction that accounts for the formation of the observed acyclic products. The formal tetraradical **7** possesses a triplet ground state and should be kinetically more stable than **6**, because strong coupling of the formally unpaired electrons at C3 and C5 reduces the through-bond interaction with the nitrene moiety that is responsible for the lability of **6**. A synthetic approach to these species requires a precursor chemistry that circumvents the intermediate formation of the labile 3-dehy-

drophenylnitrenes. Attempts in this direction are currently in progress in our laboratory.

Experimental Section

Synthesis. All phenyl azides were synthesized according to or in analogy to literature procedures starting from the corresponding anilines.²²

3-Iodo-2,4,5,6-tetrafluoronitrobenzene. H₅IO₆ (2.27 g, 10.0 mmol) was solved in 70 mL of concentrated H₂SO₄ and cooled to 0 °C. KI (4.98 g, 30.0 mmol) was added slowly with stirring. The solution was stirred for another 15 min and then 1.95 g (10 mmol) of 2,3,4,6-tetrafluoronitrobenzene was added slowly. The solution was stirred for 30 min at 0 °C and then warmed up to 50 °C for another 3.5 h. After cooling to room temperature, the solution was poured onto 500 mL of ice and extracted twice with 300 mL of MTBE. The organic phase was extracted three times with 500 mL of Na₂S₂O₃ solution (10%) and dried over MgSO₄. The solvent was removed under vacuum. After chromatographic purification (pentane) 2.95 g (9.2 mmol, 92%) of 3-iodo-2,4,5,6-tetrafluoronitrobenzene was obtained as a yellow solid.

MS (*m/z*, %) 321 (M⁺, 75), 291 (10), 263 (20), 148 (100), 117 (25), 98 (30), 69 (10). ¹³C NMR (400 MHz, [D₆]-DMSO) δ 154.3, 151.5, 149.0, 145.9, 143.2, 137.7, 135.2, 125.9, 71.7. IR (Ar, 3 K) $\tilde{\nu}/\text{cm}^{-1}$ (%) 2229.9 (5), 2196.8 (5), 2130.9 (100), 2112.4 (18), 1634.5 (10), 1492.2 (95), 1478.4 (49), 1307.6 (15), 1223.2 (31), 1012.1 (31), 1001.9 (13), 974.3 (39), 955.3 (6), 807.8 (11), 768.3 (22), 664.5 (5).

Calcd C₆F₄INO₂ (320.97): C 22.45, N 4.36. Found: C 20.26, N 5.96.

3-Iodo-2,4,5,6-tetrafluoroaniline. 3-Iodo-2,4,5,6-tetrafluoronitrobenzene (1.56 g, 8.0 mmol) was dissolved in 50 mL of methanol and 100 mg of Pt/C catalyst was added. The solution was stirred in a hydrogenator with a hydrogen pressure of 4 bar for 1 h. After the hydrogenation procedure, the catalyst was filtered off and the solvent removed. The product was purified by column chromatography (pentane) to give 800 mg (2.9 mmol, 81%) of 3-iodo-2,4,5,6-tetrafluoroaniline as a black oil.

MS (*m/z*, %) 291 (M⁺, 100), 164 (40), 148 (65), 69 (30). ¹³C NMR (400 MHz, [D₆]-DMSO) δ 146.5, 144.2, 140.6, 138.3, 137.7, 123.6, 100.1, 67.6. IR (Ar, 3 K) $\tilde{\nu}/\text{cm}^{-1}$ (%) 2229.9 (5), 2196.8 (5), 2130.9 (100), 2112.4 (18), 1634.5 (10), 1492.2 (95), 1478.4 (49), 1307.6 (15), 1223.2 (31), 1012.1 (31), 1001.9 (13), 974.3 (39), 955.3 (6), 807.8 (11), 768.3 (22), 664.5 (5).

Calcd C₆F₄INH₂ (290.99): C 24.77, N 4.81. Found: C 22.91, N 4.38.

3-Iodo-2,4,5,6-tetrafluoroazidobenzene (8). 3-Iodo-2,4,5,6-tetrafluoroaniline (0.87 g, 3.0 mmol) was dissolved in 50 mL of trifluoroacetic acid and cooled to -5 °C. Sodium nitrite (0.24 g,

(22) (a) Poe, R.; Schnapp, K.; Young, M. J. T.; Grayzar, J.; Platz, M. S. *J. Am. Chem. Soc.* **1992**, *114*, 5054. (b) Neenan, T. X.; Whitesides, G. M. *J. Org. Chem.* **1988**, *53*, 2489. (c) Filler, R.; Novar, H. *J. Org. Chem.* **1961**, *26*, 2707. (d) Kanakarajan, K.; Haider, K.; Czarnik, A. W. *Synthesis* **1988**, 566.

(23) Dunkin, I. R. *Matrix-Isolation Techniques*; Oxford University Press: Oxford, UK, 1998.

3.5 mmol), dissolved in 5 mL of water, was added slowly, keeping the temperature of the solution below 5 °C. After an additional 30 min of stirring at -5 °C, the solution was warmed to room temperature and poured onto 250 g of ice. The suspension was extracted twice with 250 mL of MTBE, and the combined organic layers were washed twice with 250 mL of a NaHCO₃ solution. The organic phase was dried over MgSO₄ and the solvent was removed under vacuum. The product was purified by column chromatography (pentane) to give 800 mg (2.5 mmol, 84%) of 3-iodo-2,4,5,6-tetrafluoroazidobenzene as a yellow oil.

MS (*m/z*, %) 317 (M⁺, 25), 289 (50), 162 (100), 148 (10), 127 (10), 93 (30), 69 (50). ¹³C NMR (400 MHz, [D₆]-DMSO) δ 150.9, 148.5, 147.5, 145.1, 144.5, 142.0, 137.0, 134.3, 114.3, 101.0, 69.0. IR (Ar, 3 K) $\tilde{\nu}/\text{cm}^{-1}$ (%) 2229.9 (5), 2196.8 (5), 2130.9 (100), 2112.4 (18), 1634.5 (10), 1492.2 (95), 1478.4 (49), 1307.6 (15), 1223.2 (31), 1012.1 (31), 1001.9 (13), 974.3 (39), 955.3 (6), 807.8 (11), 768.3 (22), 664.5 (5).

Calcd C₆F₄IN₃ (316.99): C 22.74, N 13.26. Found: C 20.45, N 14.59.

3,5-Diiodo-2,4,6-trifluoronitrobenzene. H₅IO₆ (2.27 g, 10.0 mmol) was solved in 70 mL of concentrated H₂SO₄ and cooled to 0 °C. KI (4.98 g, 30.0 mmol) was added slowly. After 15 min of stirring, 1.79 g (10 mmol) of 2,4,6-trifluoronitrobenzene was dropped slowly into the solution. After 30 min of stirring at 0 °C, the solution was warmed to 50 °C and stirred for an additional 3.5 h. After cooling to room temperature, the solution was poured onto 500 mL of ice. The aqueous solution was extracted twice with 300 mL of MTBE. The organic phase was washed three times with 500 mL of aqueous Na₂S₂O₃ (10%) and dried with MgSO₄. After removal of the solvent 3.85 g (9.0 mmol, 89%) of 3,5-diiodo-2,4,6-trifluoro-1-nitrobenzene was obtained as a yellow solid. The crude product was purified chromatographically.

MS (*m/z*, %) 429 (M⁺, 100), 399 (10), 383 (18), 272 (8), 256 (70), 129 (90), 79 (58). ¹³C NMR (400 MHz, [D₆]-DMSO) δ 70.2 (t, 28.0 Hz), 125.4 (dm, 2.9 Hz), 153.7 (d, 256.4 Hz), 156.2 (d, 248.1 Hz), 161.7 (d, 248.1 Hz). IR (Ar, 3 K) $\tilde{\nu}/\text{cm}^{-1}$ (%) 2229.9 (5), 2196.8 (5), 2130.9 (100), 2112.4 (18), 1634.5 (10), 1492.2 (95), 1478.4 (49), 1307.6 (15), 1223.2 (31), 1012.1 (31), 1001.9 (13), 974.3 (39), 955.3 (6), 807.8 (11), 768.3 (22), 664.5 (5).

Calcd C₆F₃I₂NO₂ (428.88): C 16.80, N 3.27. Found: C 16.63, N 3.90.

3,5-Diiodo-2,4,6-trifluoroaniline. 3,5-Diiodo-2,4,6-trifluoronitrobenzene (1.29 g, 3.0 mmol) was dissolved in 50 mL of methanol and 100 mg of Pt/C was added. This solution was stirred in a hydrogenator with a H₂ pressure of 4 bar for 1 h. After hydrogenation, the catalyst was separated and the solvent removed. After purification by column chromatography (pentane), 1.03 g (2.6 mmol, 86%) of 3,5-diiodo-2,4,6-trifluoroaniline was obtained as a bright yellow solid.

MS (*m/z*, %) 399 (M⁺, 100), 272 (30), 145 (60), 117 (20), 99 (20), 70 (10). ¹³C NMR (400 MHz, [D₆]-DMSO) δ 151.4, 149.1, 66.2. IR (Ar, 3 K) $\tilde{\nu}/\text{cm}^{-1}$ (%) 2229.9 (5), 2196.8 (5), 2130.9 (100), 2112.4 (18), 1634.5 (10), 1492.2 (95), 1478.4 (49), 1307.6 (15), 1223.2 (31), 1012.1 (31), 1001.9 (13), 974.3 (39), 955.3 (6), 807.8 (11), 768.3 (22), 664.5 (5).

Calcd C₆F₃I₂NH₂ (398.89): C 18.07, N 3.51. Found: C 18.28, N 3.58.

3,5-Diiodo-2,4,6-trifluorophenyl Azide (9). 3,5-Diiodo-2,4,6-trifluoroaniline (0.7 g, 1.8 mmol) was dissolved in 50 mL of trifluoroacetic acid and cooled to -5 °C. Sodium nitrite (0.2 g, 3 mmol), dissolved in 5 mL of H₂O, was added within 15 min, while the temperature of the solution was kept below 5 °C. After 30 min of stirring at -5 °C, a solution of 0.2 g (3 mmol) of sodium azide in 5 mL of water was added slowly and the solution was stirred subsequently for an additional 30 min. After warming to room temperature, it was poured onto 250 g of ice and extracted twice with 250 mL of MTBE. The organic phase was extracted twice with 250 mL of a diluted NaHCO₃ solution and the procedure

repeated with saturated NaHCO₃ solution. The organic phase was dried over MgSO₄ and the solvent was removed in vacuum. The product was purified by column chromatography (pentane) to yield 650 mg (1.5 mmol) of 3,5-diiodo-2,4,6-trifluoro-1-azidobenzene as a bright yellow solid.

MS (*m/z*, %) 425 (M⁺, 25), 397 (60), 270 (100), 143 (55), 124 (50), 93 (40), 69 (10). ¹³C NMR (400 MHz, [D₆]-DMSO) δ 158.5, 156.1, 153.6, 113.5, 68.2. IR (Ar, 3 K) $\tilde{\nu}/\text{cm}^{-1}$ (%) 2229.9 (5), 2196.8 (5), 2130.9 (100), 2112.4 (18), 1634.5 (10), 1492.2 (95), 1478.4 (49), 1307.6 (15), 1223.2 (31), 1012.1 (31), 1001.9 (13), 974.3 (39), 955.3 (6), 807.8 (11), 768.3 (22), 664.5 (5).

Calcd C₆F₃I₂N₃ (424.89): C 16.96, N 9.89. Found: C 16.84, N 10.67.

Matrix Isolation. Matrix isolation experiments were performed by standard techniques²² with closed cycle helium cryostats allowing cooling of a CsI spectroscopic window to 3 or 10 K, respectively. FTIR spectra were recorded with a standard resolution of 0.5 cm⁻¹, using a N₂(*l*)-cooled MCT detector in the range 400–4000 cm⁻¹. X-band EPR spectra were recorded from a sample deposited on an oxygen-free high-conductivity copper rod (75 mm length, 2 mm diameter) cooled by a closed-cycle cryostat.

Broadband irradiation was carried out with mercury high-pressure arc lamps in housings equipped with quartz optics and dichroic mirrors in combination with cutoff filters (50% transmission at the wavelength specified). IR irradiation from the lamps was absorbed by a 10 cm path of water. For 254 nm irradiation a low-pressure mercury arc lamp was used. A XeCl Excimer Laser was used for 308 nm, and a KrF Excimer Laser for 248 nm irradiation.

Computational Methods. Optimized geometries and vibrational frequencies of all species were calculated at the BLYP level²⁴ employing the 6-311G(d,p) polarized valence-triple- ξ basis set.²⁵ Tight convergence criteria for gradients and a full (99 590) integration grid, having 99 radial shells per atom and 590 angular points per shell, were used throughout. Despite the neglect of relativistic effects, this approach has been shown to reproduce the measured IR spectra of several iodoaromatic compounds accurately.^{11,20c,e} A spin-unrestricted formalism was used for all high-spin systems and for singlet biradicals, whenever an external instability²⁶ was observed. All DFT calculations were carried out with Gaussian 98.²⁷ The GAMESS-US program package was used

(24) (a) Becke, A. D. *Phys. Rev. A* **1988**, *38*, 3098. (b) Lee, C.; Yang, W.; Parr, R. G. *Phys. Rev. B* **1988**, *37*, 785.

(25) (a) Glukhovstev, M. N.; Pross, A.; McGrath, M. P.; Radom, L. *J. Chem. Phys.* **1995**, *103*, 1878. (b) Basis sets were obtained from the Extensible Computational Chemistry Environment Basis Set Database, Version 6/19/03, as developed and distributed by the Molecular Science Computing Facility, Environmental and Molecular Sciences Laboratory, which is part of the Pacific Northwest Laboratory, P.O. Box 999, Richland, Washington 99352, and funded by the U.S. Department of Energy. The Pacific Northwest Laboratory is a multiprogram laboratory operated by Battelle Memorial Institute for the U.S. Department of Energy under contract DE-AC06-76-RLO 1830. Contact David Feller or Karen Schuchardt for further information.

(26) Bauernschmitt, R.; Ahlrichs, R. *J. Chem. Phys.* **1996**, *104*, 9047.

(27) Frisch, M. J.; Trucks, G. W.; Schlegel, H. B.; Scuseria, G. E.; Robb, M. A.; Cheeseman, J. R.; Zakrzewski, V. G.; Montgomery, J. A., Jr.; Stratmann, R. E.; Burant, J. C.; Dapprich, S.; Millam, J. M.; Daniels, A. D.; Kudin, K. N.; Strain, M. C.; Farkas, O.; Tomasi, J.; Barone, V.; Cossi, M.; Cammi, R.; Mennucci, B.; Pomelli, C.; Adamo, C.; Clifford, S.; Ochterski, J.; Petersson, G. A.; Ayala, P. Y.; Cui, Q.; Morokuma, K.; Malick, D. K.; Rabuck, A. D.; Raghavachari, K.; Foresman, J. B.; Cioslowski, J.; Ortiz, J. V.; Stefanov, B. B.; Liu, G.; Liashenko, A.; Piskorz, P.; Komaromi, I.; Gomperts, R.; Martin, R. L.; Fox, D. J.; Keith, T.; Al-Laham, M. A.; Peng, C. Y.; Nanayakkara, A.; Gonzalez, C.; Challacombe, M.; Gill, P. M. W.; Johnson, B.; Chen, W.; Wong, M. W.; Andres, J. L.; Gonzalez, C.; Head-Gordon, M.; Replogle, E. S.; Pople, J. A. *Gaussian 98*; Gaussian, Inc.: Pittsburgh, PA, 1998.

(28) Schmidt, M. W.; Baldrige, K. K.; Boatz, J. A.; Elbert, S. T.; Gordon, M. S.; Jensen, J. H.; Koseki, S.; Matsunaga, N.; Nguyen, K. A.; Su, S. J.; Windus, T. L.; Dupuis, M.; Montgomery, J. A. *J. Comput. Chem.* **1993**, *14*, 1347.

(29) Dunning, T. H. *J. Chem. Phys.* **1989**, *90*, 1007.

for ab initio calculations.²⁸ The active spaces for CASSCF calculations cover the six valence π orbitals, and the formally singly occupied radical orbitals at nitrogen or carbon, resulting in (8,8) active spaces for **30** and **31**, (9,9) for **29**, and (10,10) for **28**. Harmonic vibrational frequencies were computed by finite differences of analytic first derivatives for the lowest energy state within a given spin multiplicity. Subsequent multireference second-order perturbation theory single-point energy computations (MRMP2)¹⁹ were performed within the frozen core approximation, using the same active spaces. Dunning's cc-pVTZ basis set with spherical harmonic polarization functions was employed in all computations.²⁹

Acknowledgment. This work was financially supported by the Deutsche Forschungsgemeinschaft and the Fonds der Chemischen Industrie.

Supporting Information Available: Calculated IR spectra and energies of various potential photoproducts, IR spectroscopic data of **10–13**, as well as CASSCF geometries of low-lying states of **28**. This material is available free of charge via the Internet at <http://pubs.acs.org>.

JO061624B